Fluorescence and Conformational Stability Studies of *Staphylococcus* Nuclease and Its Mutants, Including the Less Stable Nuclease–Concanavalin A Hybrids†

Maurice R. Eftink*

Department of Chemistry, University of Mississippi, University, Mississippi 38677

Camillo A. Ghiron

Department of Biochemistry, University of Missouri, Columbia, Missouri 65201

Roger A. Kautz‡ and Robert O. Fox‡,§

Department of Molecular Biophysics and Biochemistry and The Howard Hughes Medical Institute, Yale University, New Haven, Connecticut 06511

Received June 18, 1990; Revised Manuscript Received October 16, 1990

ABSTRACT: We report steady-state and time-resolved fluorescence studies with the single tryptophan protein, *Staphylococcus aureus* A, and several of its site-directed mutants. A couple of these mutants, nuclease–conA and nuclease–conA–S28G (which are hybrid proteins containing a six amino acid β-turn substitute from concanavalin A), are found to have a much lower thermodynamic stability than the wild type. The thermal transition temperatures for nuclease–conA and S28G are 32.8 and 30.5 °C, which are about 20 °C lower than the T_m for wild-type nuclease A. These mutant proteins also are denatured by a much lower concentration of the denaturants urea and guanidine hydrochloride. We also show that an unfolding transition in the structure of the nuclease–conA hybrids can be induced by relatively low hydrostatic pressure (~700 bar). The free energy for unfolding of nuclease–conA (and nuclease–conA–S28G) is found to be only 1.4 kcal/mol (and 1.2 kcal/mol) by thermal, urea, guanidine hydrochloride, and pressure unfolding. Time-resolved fluorescence intensity and anisotropy measurements with nuclease–conA–S28G show the temperature-, urea-, and pressure-perturbed states each to have a reduced average intensity decay time and to depolarize with a rotational correlation time of ~1.0 ns (as compared to a rotational correlation time of 11 ns for the native form of nuclease–conA–S28G at 20 °C).

Site-directed mutagenesis provides a means of selectively substituting particular amino acids in proteins and thus for perturbing and studying the functional, structural, thermodynamic, and dynamic properties of proteins (Oxender & Fox, 1987; Matthews, 1987; Becktel & Schellman, 1987; Kellis et al., 1988; Kitamura & Sturtevant, 1989; Borgford et al., 1987).

The intrinsic fluorescence of tryptophan (Trp) residues in proteins is a valuable probe for studying the solution structure and dynamics of proteins (Beechem & Brand, 1985). Using mutagenesis techniques to insert/delete specific Trp residues (or residues near Trp), several groups have recently performed such fluorescence studies to characterize various properties of proteins (Hudson et al., 1988; Rudzki et al., 1986; Waldman et al., 1987; Hansen et al., 1987; Eftink et al., 1989).

Here we report studies of the intrinsic fluorescence of Trp-140 in the wild type and specific mutants of nuclease A from *Staphylococcus aureus*. A variety of specific mutants of this protein have been prepared and several important biophysical investigations have been performed with these mutants (Shortle et al., 1988; Fox et al., 1986; Evans et al., 1987; Hynes et al., 1989; Serpersu et al., 1988; Alexandrescu et al., 1989). The fluorescence of the single Trp-140 of nuclease A has been previously studied (Lakowicz et al., 1986; Brochon et al., 1974; Grinvald & Steinberg, 1976). A double-exponential decay is needed to describe the fluorescence of this residue. Trp-140 lies near the surface of the protein (Cotton & Hazen, 1971). Anisotropy decay studies indicate a small degree of independent motion of this residue, with the major rotational correlation time being that for global rotation of the protein (Lakowicz et al., 1986; Eftink et al., 1990).

The present studies employ a series of six mutants prepared primarily for a study of the kinetics of protein folding and refolding (i.e., mostly proline substitutions) (Evans et al., 1987; Hynes et al., 1989; Antonino et al., 1989). The fluorescence properties of most of the mutants are found to be very similar to those of the wild type. Two of the mutants are found to have a significantly reduced structural stability. These unstable mutants are hybrid proteins that possess a six amino acid type I β-turn sequence in place of a five-residue (Tyr-Lys-Gly-Gln-Pro, residues 27–31) type I′ β-turn in the wild type; in nuclease–conA the transferred hexapeptide, Ser-Ser-Asn-Gly-Ser-Pro, is identical with a segment of concanavalin A (Hynes et al., 1989), and in nuclease–conA–S28G the second Ser of the above sequence is substituted by Gly. These latter two hybrid proteins were originally prepared to test the ability to transfer elements of secondary structure from one protein to another as a strategy in protein engineering. X-ray crystallographic studies show the hybrid, nuclease–conA, to have a similar overall structure to the wild type.

This article presents a survey of the fluorescence properties and thermodynamic stability of these mutant and hybrid forms of nuclease A. Thermal, solvent, and pressure unfolding studies are presented. Elsewhere we will present more detailed

† This research was supported by NSF Grant DMB 88-06113 to M.R.E. and NIH Grant R01 AI23923 to R.O.F. A preliminary report of this work appears in SPIE Proceedings (Eftink et al., 1990). In this preliminary report, nuclease–conA–S28G was inadvertently referred to as P56A.

‡ Department of Molecular Biophysics and Biochemistry.

§ The Howard Hughes Medical Institute.

0006-2960/91/0430-1193$02.50/0

studies of the fluorescence decay and anisotropy decay of one of the mutants, nuclease–conA–S28G, and the wild-type nuclease A.

Experimental Section

Materials. Nuclease mutants P117G, P117T, K116G, H124L, and the two hybrid nuclease–conA proteins and wild-type nuclease were isolated and purified as described elsewhere (Kautz et al., 1990) from *Escherichia coli* that contained recombinant nuclease genes. The gene was cloned from *S. aureus* Foggi stain and was introduced by the vector pAS1. Mutant genes were prepared via oligonucleotide-directed mutagenesis. The proteins were purified by using a phosphocellulose column. SDS–polyacrylamide gel electrophoresis was run on nuclease–conA–S28G and the wild type. These proteins were found to be >97% pure, as stained by Coomassie blue.

Acrylamide was recrystallized from ethyl acetate before use. Urea was recrystallized from ethanol and guanidine hydrochloride was grade I from Sigma Chemical Co.

Proteins were dissolved in either a buffer of 0.01 M Tris-HCl and 0.1 M NaCl, pH 7.0, or a buffer of 0.05 M sodium acetate, pH 5.3.

Methods. Steady-state fluorescence measurements were made with a Perkin-Elmer MPF 44A fluorometer. The sample holder was thermojacketed. In thermal denaturation studies, temperature in the sample cuvette was measured with a thermistor probe, as the temperature was increased at a rate of about 0.5 °C/min. Excitation and emission wavelengths of 295 and 320 nm were used (i.e., the blue side of the emission was observed to maximize the signal change upon unfolding). The excitation shutter was closed, when measurements were not being made, to minimize photolysis. Samples having an absorbance at 295 nm of about 0.02 were used for the unfolding studies.

The apparent enthalpy change, $\Delta H°_{app}$, entropy change, $\Delta S°_{app}$, and melting temperature, T_m, for the thermal transitions were determined by fitting the following equation,

$$F(T) = [1 - f_U(T)][F_{N,0} - S_N \cdot T] + f_U(T)[F_{U,0} - S_U \cdot T] \quad (1a)$$

where

$$f_U(T) = \exp(-\Delta G°_{UN}(T)/RT)/[1 + \exp(-\Delta G°_{UN}(T)/RT)] \quad (1b)$$

and

$$\Delta G°_{UN}(T) = \Delta H°_{UN,app} - T\Delta S°_{UN,app} \quad (1c)$$

and where $F(T)$ is the observed fluorescence signal at any temperature, $F_{N,0}$ and $F_{U,0}$ are the fluorescence intensities of the native (N) and unfolded (U) state at 0 °C, and S_N and S_U are the temperature dependencies of the fluorescence of the N and U states (i.e., S_N is the slope of F versus T for the N state before the transition). This fitting procedure follows that described by Shortle et al. (1988). We used the nonlinear least-squares program ENZFITTER (BIOSOFT Co.) to fit data (see Figure 2) for $\Delta H°_{UN,app}$, $\Delta S°_{UN,app}$, $F_{N,0}$, $F_{U,0}$, and S_N (usually we assumed a value of S_U, as the fit is insensitive to this parameter).

Solvent denaturation by urea and guanidine hydrochloride was also experimentally measured by steady-state fluorescence. Aliquots of 10 M urea or 8 M guanidine were added to a sample. (In cases where high denaturant concentration was needed, a Job method was used.) After corrections for dilution of the sample, the fluorescence data were fitted with the eq 2, which assumes the linear dependence of $\Delta G°_{UN}(d)$ on denaturant concentration (Pace et al., 1989; Schellman, 1978).

$$F(d) = [1 - f_U(d)][F_{N,0} - S_N \cdot [d]] + f_U(d)[F_{U,0} - S_U[d]] \quad (2a)$$

where

$$f_U(d) = \exp(-\Delta G°_{UN}(d)/RT)/[1 + \exp(-\Delta G°_{UN}(d)/RT)] \quad (2b)$$

and

$$\Delta G°_{UN}(d) = \Delta G°_{UN} - m[d] \quad (2c)$$

That is, the apparent free energy of unfolding, $\Delta G°_{UN}(d)$, is assumed to be equal to the $\Delta G°_{UN}$ value in the absence of denaturant minus m·[d], where m is an index of responsiveness of the protein to unfolding by the denaturant (equation 2c) and [d] is the molar concentration of the denaturant. Here S_N and S_D are the slopes of the fluorescence intensity versus [d] for the N and D states and $F_{N,0}$ and $F_{U,0}$ are the fluorescence intensities of the native and unfolded states in the absence of denaturant. As with the fitting with eq 1, a nonlinear least-squares routine was used to obtain $\Delta G°_{UN}$, $F_{N,0}$, $F_{U,0}$, m, and S_D (the value of S_N was fixed at zero, since the fit is insensitive to this parameter).

Fluorescence lifetime and anisotropy decay measurements were performed with a multifrequency (1–200 MHz) phase fluorometer (hybrid from SLM-Aminco, Inc., Urbana, IL, and ISS Inc., Urbana, IL), as described elsewhere (Eftink & Ghiron, 1987). A 15-W argon ion laser (Coherent, Palo Alto, CA) was used to excite the samples with a line at 300 nm.

Pressure-induced unfolding studies were performed with a high-pressure chamber from ISS Inc. We found phase angle measurements to be more stable than either relative modulation or intensity measurements. The phase angle of a reference sample (*p*-terphenyl in ethanol, 1.0-ns lifetime) was measured before and after a pressure run. The protein sample was placed in the chamber (in a small quartz bottle, with a pliable plastic top to act as a pressure transducer) and fluorescence measurements were made as a function of pressure. Typically we started by pressurizing the chamber to about 2000 bar and made measurements in a descending manner. The phase angle versus pressure data were found to be reversible.

For the nuclease–conA hybrids, phase angle versus pressure data were described in terms of a two-state (N $\rightleftarrows$ U) unfolding transition by using the following equation. Here $\Theta(P)$ is the observed relative phase angle at any pressure, P, $\Theta_{N,0}$ and $\Theta_{U,0}$ are the phase angles of the N and U states at 1 atm, S_N and S_U are the pressure dependencies of the Θ_N and Θ_U values for the two separate states, $\Delta G°_{UN}$ is the free energy change for the unfolding transition at 1 atm (and the experimental temperature), and $\Delta V°$ is the volume change for the transition (P is in bar or atmospheres).

$$\Theta(P) = [1 - f_U(P)][\Theta_{N,0} - S_N \cdot P] + f_U(P)[\Theta_{U,0} - S_U \cdot P] \quad (3a)$$

$$f_U(P) = \exp(-\Delta G°_{UN}(P)/RT)/[1 + \exp(-\Delta G°_{UN}(P)/RT)] \quad (3b)$$

$$\Delta G°_{UN}(P) = \Delta G°_{UN} + P\Delta V° \cdot R/82 \quad (3c)$$

A nonlinear least-squares fit was obtained by setting S_N and S_U to be equal to zero (i.e., no intrinsic pressure dependence for the individual states; we included S_N and S_U in eq 3 only for the sake of completion) and by fitting for $\Theta_{N,0}$, $\Theta_{U,0}$, $\Delta G°_{UN}$, and $\Delta V°$.

Fluorescence lifetime measurements at high pressures were made by first recording the frequency dependence of the phase

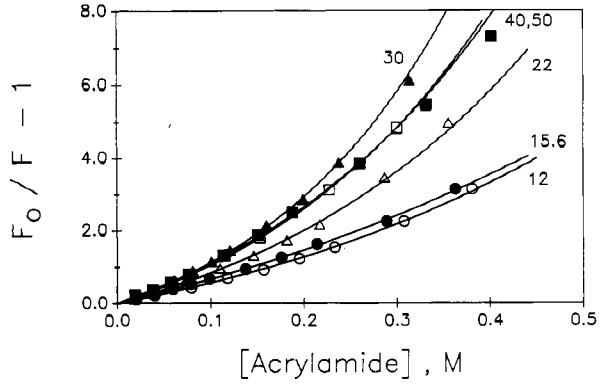

FIGURE 1: Stern–Volmer plots for the acrylamide quenching of the steady-state fluorescence of the nuclease–conA–S28G mutant as a function of temperature: (○) 12 °C; (●) 15.6 °C; (△) 22 °C; (▲) 30 °C; (□) 40 °C; (■) 50 °C.

angle and modulation for *p*-terphenyl in a quartz bottle in the pressure cell at 1 atm and then performing similar frequency-dependent measurements for the pressurized protein sample. Measuring the reference and sample signals about 15 min apart does introduce some uncertainty, but the excellent stability of the Pockells cell and the dramatic change in lifetime upon unfolding make these measurements possible. Differential phase/modulation anisotropy decay measurements of the pressurized sample were made on the protein sample alone. No correction was necessary for the pressure dependence of the birefringence of the cell's quartz windows, since the frequency dependence of the difference phase/modulation data and not the absolute value of the anisotropy (i.e., the r_0) is critical in our data analysis.

Results

Steady-State Emission Spectra and Acrylamide Quenching. The emission spectra of the group of nuclease mutants were found to be nearly identical, with a maximum around 335 nm. Acrylamide quenching studies were performed to estimate the accessibility of Trp-140 in the group of mutants. Again, the proteins appeared similar, with an effective acrylamide (Stern–Volmer) quenching constant of 5–6 M^{-1} (dynamic and static quenching constants of 4.5 and 1.0 M^{-1}, respectively, for the wild type, for example).

For nuclease–conA–S28G, a mutant having a hexapeptide, β-turn sequence substituted at position 27–31, the acrylamide quenching profile was found to be extremely temperature sensitive, as illustrated in Figure 1. As the temperature was increased from 15 to 30 °C, the effective quenching constant increased by 50% and a marked upward curvature was observed. Above 30 °C, the effective quenching constant decreased slightly. This pattern suggests that nuclease–conA–S28G has a very low T_m and that acrylamide can induce the unfolding of the protein at temperatures near T_m.

Thermal Unfolding. In view of the above indication of a low T_m for nuclease–conA–S28G, we studied the thermal unfolding of the series of nuclease mutants, by measuring fluorescence versus temperature as previously done by Shortle et al. (1988) for other nuclease mutants. Shown in Figure 2 are thermal unfolding data for nuclease–conA–S28G, nuclease–conA, and the wild type. The apparent enthalpy change for unfolding, $\Delta H°_{UN,app}$, and the melting temperature, T_m, are listed in Table I. For comparison, the data of Shortle et al. are included. (Their buffers contained phosphate and ours did not; this may account for the small difference we find for the wild type, since phosphate may slightly stabilize the protein. No calcium was added in either study.) Thermal unfolding

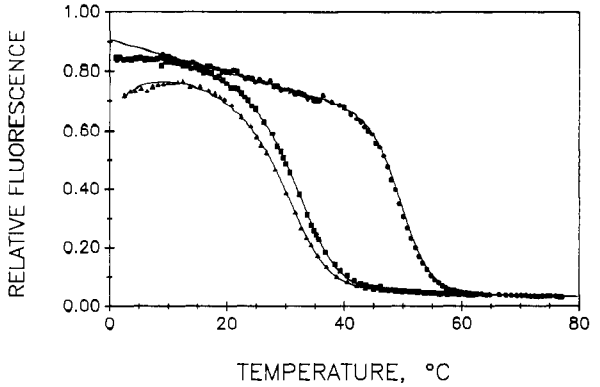

FIGURE 2: Thermal–fluorescence transitions for nuclease–conA–S28G (▲), nuclease–conA (■), and wild-type (●) nuclease. Solid lines are fits to eq 1 with the $\Delta H°_{app}$ and T_m values in Table I. The values for the other fitting parameters in eq 1 are, for wild type, $F_{N,0} = 0.9076$, $F_{U,0} = 0.0592$, $S_N = 0.0055$, and $S_U = 3.1 \times 10^{-4}$. For nuclease–conA–S28G and nuclease–conA, eq 4 was used for the temperature-dependent $\Delta G°_{UN}(T)$; this equation includes the possibility of cold denaturation. The fit for nuclease–conA–S28G is for $\Delta H°_{UN} = 45.79$ kcal/mol, $\Delta C_p = 2.68$ kcal/(mol·deg), $T_m = 30.1$ °C, $F_{N,0} = 0.904$, and $F_{U,0} = 0.102$. (S_U and S_N are assumed to have the same values as for wild-type nuclease.) For nuclease–conA, the fit is for $\Delta H°_{UN} = 48.4$ kcal/mol, $\Delta C_p = 2.33$ kcal/(mol·deg), $T_m = 32.2$ °C, $F_{N,0} = 0.938$, and $F_{U,0} = 0.0669$ (and with S_U and S_N fixed as 3×10^{-4} and 5.5×10^{-3}).

Table I: Thermodynamic Values for the Thermal Unfolding of Nuclease and Its Mutants[a]

protein	T_m (°C)	$\Delta H°_{app}$ (kcal/mol)	ref
wild type (w/o P_i)[b]	50.6	82.6	this work
wild type (w P_i)[c]	52.1	79.9	this work
P117G	55.6	91.9	this work
P117T	51.2	71.7	this work
H124L	56.4	92.0	this work
K116G	54.4	86.9	this work
nuclease–conA	32.8	48.7	this work
nuclease–conA–S28G	30.5	45.9	this work
nuclease–conA–S28G (pH 5.3)[d]	26.0	43.1	this work
wild type (w P_i)[e]	53.4	88.8	Shortle et al. (1988)
V66L	55.7	72.3	Shortle et al. (1988)
V66L + G88V	57.6	56.0	Shortle et al. (1988)
G88V	55.9	68.9	Shortle et al. (1988)
V66L + G79S + G88V	53.4	44.0	Shortle et al. (1988)
A69T	41.2	63.4	Shortle et al. (1988)
I18M + A90S	41.6	72.5	Shortle et al. (1988)

[a] Values obtained at pH 7.0, 0.01 M Tris-HCl, and 0.1 M NaCl, unless stated otherwise. $\Delta H°_{app}$ and $\Delta S°_{app}$ are values at $T = T_m$. [b] Indicates the absence of phosphate. [c] Buffer was 0.02 M sodium phosphate, pH 7.2. [d] Buffer was 0.05 M sodium acetate, pH 5.3. [e] All studies from Shortle et al. (1988) were in 0.025 M sodium phosphate and 0.1 M NaCl, pH 7.0.

of nuclease A is known to be reversible in the pH range studied (Shortle et al., 1988). We have found no evidence for irreversible behavior for any of the proteins studied here.

Many of the mutants have a T_m slightly above that for the wild type (51 °C). The hybrid nuclease–conA and nuclease–conA–S28G proteins, however, have a remarkably lower T_m of 32.8 and 30.5 °C, respectively. The $\Delta H°_{UN,app}$ is also smaller for these two hybrid proteins.

The free energy of unfolding at 20 °C, $\Delta G°_{UN}(T = 20°)$, can be estimated from the $\Delta H°_{UN,app}$ and T_m values for the various proteins by the relationship (Pace et al., 1989; Schellman, 1978)

$$\Delta G°_{UN}(T) = \Delta H°_{UN,app}(1 - T/T_m) - \Delta C_p[(T_m - T) + T \ln (T/T_m)] \quad (4)$$

To evaluate $\Delta G°_{UN}$, a value for the heat capacity change for unfolding, ΔC_p, must also be known or assumed. From measurements of $\Delta H°_{UN,app}$ at various pHs, Shortle et al.

Table II: Free Energy Change and Other Thermodynamic Parameters for the Unfolding of Nuclease and the Hybrid Mutants[a]

	$\Delta G°_{UN}$ at 20 °C (kcal/mol)			
	thermal	urea	Gu·HCl	pressure
wild type	5.76	6.11 ± 0.50	5.50 ± 0.30	
nuclease-conA	1.76		1.20[b]	1.26 ± 0.16
nuclease-conA-S28G	1.37	0.86 ± 0.20	1.27 ± 0.30	1.25 ± 0.16
$\Delta\Delta G°_{UN}$(WT nuclease-conA)	4.00		4.30	
$\Delta\Delta G°_{UN}$(WT nuclease-conA-S28G)	4.39	5.25	4.23	

	$\Delta H°_{app}$ (kcal/mol)	m_{urea} (kcal/mol)	$m_{Gu.HCl}$ (kcal/mol)	$\Delta V°$ (mL/mol)
wild type	82.6 ± 0.5	−2.63 ± 0.40	−5.67 ± 0.50	
nuclease-conA	48.7 ± 0.6		−8.57[b]	−137 ± 15
nuclease-conA-S28G	45.9 ± 0.7	−2.58 ± 0.25	−9.10 ± 0.40	−124 ± 15

[a] Values for pH 7, 0.01 M Tris-HCl, and 0.1 M NaCl. $\Delta G°_{UN}$ values calculated from eq 4 or from fits to eqs 2 and 3. [b] Value from Hynes et al. (1989).

(1988) determined ΔC_p = 1000 cal/(mol·deg) for wild-type nuclease A. From our $\Delta H°_{app}$ values at pH 5.3 and 7.0 we calculate ΔC_p = 850 cal/(mol·deg) for nuclease-conA-S28G. From these ΔC_p values, the $\Delta G°_{UN}$ at 20 °C for the wild type is estimated to be 5.76 kcal/mol and the $\Delta G°_{UN}$ at 20 °C for nuclease-conA-S28G is estimated to be 1.37 kcal/mol. Thus, substitution of the peptide at residues 27–31 results in a destabilization of nuclease by over 4 kcal/mol.

The other unstable mutant protein, nuclease-conA, is found to also have a $\Delta G°_{UN}$ of 1.76 kcal/mol [assuming a ΔC_p value of 1000 cal/(mol·deg).

The fluorescence thermal profile for nuclease-conA-S28G shows a slight increase in fluorescence intensity as temperature is increased from 0 to 15 °C (positive initial slope). By contrast, the intensity of the wild type's fluorescence decreases in a linear manner with an increase in temperature from 10 to 40 °C (negative slope). This latter temperature dependence is the expected pattern. The positive initial slope for nuclease-conA-S28G is an abnormal temperature dependence of the fluorescence of a tryptophan residue, as it implies a negative activation energy for quenching reactions. An alternate explanation for the positive initial slope for nuclease-conA-S28G is that the fluorescence below 15 °C monitors the cold denaturation of the protein. The cold denaturation process can, in principle, be described by using eq 4, instead of eq 1c, in the fitting routine. Equation 4 differs from eq 1c by inclusion of the heat capacity change, ΔC_p. By substituting eq 4 into the fit of eqs 1a–b, we obtain the solid curve fit in Figure 1 for the unfolding of nuclease-conA-S28G. This fit is for $\Delta H°_{app}$ = 45.79 kcal/mol and ΔC_p = 2.68 kcal/(mol·deg). Thus the initial positive slope for nuclease-conA-S28G can be described by the cold denaturation phenomenon, with the protein being maximally stable at 13.5 °C and with the fluorescence intensity dropping above and below this temperature due to "cold" and "hot" denaturation. The fitted ΔC_p is larger than expected, but the fit requires the assumption that the temperature dependence of the intensity of the native state, S_N, is the same for nuclease-conA-S28G as it is for the wild type (for which S_N is well defined).

The data for nuclease-conA are also well fitted by the cold unfolding model, as shown by the solid curve through the data in Figure 1.

Solvent Unfolding. Shown in Figure 3 are data for the fluorescence intensity of nuclease-conA-S28G and wild-type nuclease as a function of the concentration of urea and guanidine hydrochloride at 20 °C. As expected from the low T_m of nuclease-conA-S28G, this mutant is unfolded by very low concentrations of urea (C_m = 0.33 M) and guanidine hydrochloride (C_m = 0.16 M). By fitting eq 2 to these data, values for the free energy of unfolding at 20 °C, $\Delta G°_{UN}$, and the parameter m were obtained and are listed in Table II.

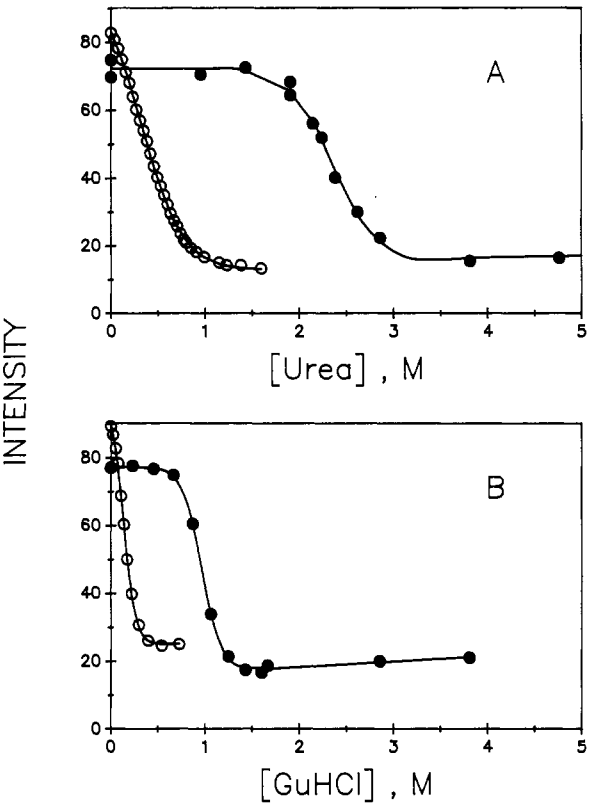

FIGURE 3: (A) Urea denaturation of nuclease-conA-S28G (○) and wild-type nuclease (●). Solid lines are fits to eq 2 with the $\Delta G°_{UN}$ and m values given in Table II. Data taken at 20 °C. S_N is assumed to be equal to zero; S_U is assumed to be the same for wild type and nuclease-conA-S28G. (B) Guanidine hydrochloride denaturation of nuclease-conA-S28G and wild-type nuclease. Solid lines are fits to eq 2 with the $\Delta G°_{UN}$ and m values given in Table II. Data taken at 20 °C. S_N and S_U treated as above.

(Note that we have performed a nonlinear least-squares fit of eq 2 directly to the F(d) versus [d] data, rather than constructing linear plots of $-RT \ln K_{UN}$ versus [d]. The nonlinear regression fits do not require prior estimations of F_N and F_U.) $\Delta G°_{UN}$ values of 0.86 and 1.27 kcal/mol were determined for nuclease-conA-S28G by using urea and guanidine hydrochloride as denaturants at 20 °C. Values of $\Delta G°_{UN}$ for the wild type were obtained in a similar manner and are also listed in Table III, together with the $\Delta G°_{UN}$ obtained from thermal unfolding. The excellent fits of eq 2 to the data in Figure 3 support the assumption that the urea and guanidine hydrochloride unfolding processes are two-state transitions [i.e., although not shown, plots of ln K_{UN} versus [d] are linear (Shortle & Meeker, 1986)].

Pressure Unfolding. With a modulation frequency of 50 MHz, the phase angle of the fluorescence of nuclease-conA-

Table III: Fluorescence Decay Fitting Parameters for Nuclease–conA–S28G[a]

	double exponential				Lorentzian distrib		
temp (°C)	τ_1	τ_2	α_1	χ^2_R	$\bar{\tau}$	Γ	χ^2_R
3.3	1.13	6.11	0.056	2.13	5.84	1.72	3.02
10.3	2.22	6.10	0.205	1.70	5.78	1.07	1.82
19.9	1.87	5.75	0.282	1.02	5.26	1.51	1.18
24.6	1.81	5.48	0.318	1.26	4.91	1.57	1.83
29.8	1.37	5.08	0.430	4.10	4.20	2.31	3.97
34.5	0.98	4.34	0.577	3.87	3.00	2.87	3.30
39.6	0.77	3.29	0.635	13.2	2.05	2.41	9.47
49.8	0.45	2.02	0.625	4.00	1.32	1.37	5.33
59.7	0.42	1.69	0.716	13.6	0.93	1.10	11.02
1.5 M urea, 20 °C	1.0	4.16	0.585	3.88	2.86	2.80	4.78
1333 bar, 20 °C	0.71	3.03	0.460	97.3	2.87	2.65	113.4

[a] Buffer was 0.01 M Tris-HCl and 0.1 M NaCl, pH 7.0. χ^2_R is based on values of $\sigma_p = 0.2°$ and $\sigma_M = 0.004$ for all experiments, except the high-pressure measurement for which $\sigma_p = 0.3°$ and $\sigma_M = 0.010$ was used.

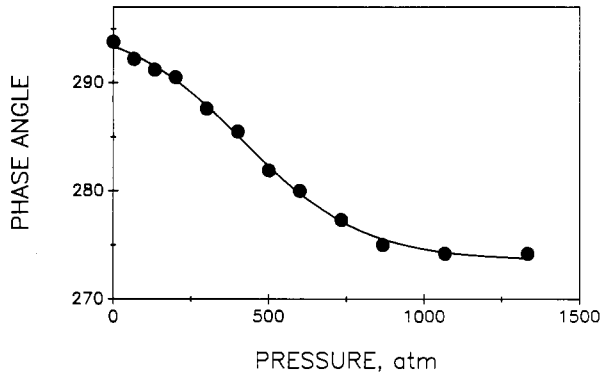

FIGURE 4: Pressure denaturation of nuclease–conA–S28G at 21 °C, pH 7. The ordinant is the raw phase angle (50-MHz modulation frequency). The solid line is a fit of eq 3 with the $\Delta G°_{UN}$ and $\Delta V°$ values in Table II. Other fitting parameters are $\Theta_N = 295.7°$ and $\Theta_U = 273.5°$; S_N and S_U were assumed to be equal to zero.

S28G was measured as a function of hydrostatic pressure at 20 °C. As shown in Figure 4, the phase angle of nuclease–conA–S28G decreases as pressure is increased from 1 to 2000 bar. This decrease in phase angle corresponds to a decrease in fluorescence phase lifetime from approximately 5 to 1 ns. The emission spectrum also red shifts and lowers in intensity with the transition. The decrease in phase angle data were analyzed with eq 3 to obtain a volume change, $\Delta V°$, for the transition of −124 ml/mol and a $\Delta G°_{UN} = 1.25$ kcal/mol at 21 °C. This $\Delta V°$ value should be considered to be an apparent value, as it has not been corrected for contributions from protonic equilibria shifts upon unfolding and consequent protonation/deprotonation of the Tris buffer [see Zipp and Kauzmann (1973) for a complete study of the pressure unfolding of proteins].

By comparison, the phase angle of the wild-type nuclease remains constant from 1 to 3000 bar and thus shows no transition in this pressure range. Studies with nuclease–conA gave a pressure transition that is similar to that for nuclease–conA–S28G. The data for nuclease–conA were fitted with $\Delta V° = -137$ mL/mol and $\Delta G°_{UN} = 1.26$ kcal/mol.

The pressure-induced decrease in fluorescence lifetime for nuclease–conA–S28G is similar to the drop in lifetime caused by thermal denaturation and urea denaturation (see below).

Fluorescence Lifetime Data. More extensive fluorescence lifetime data will be provided for nuclease–conA–S28G and wild-type nuclease in a separate paper (Eftink et al., 1991). Here we will present fluorescence lifetime data for nuclease–conA–S28G and the wild-type protein as they are perturbed by temperature, urea, and pressure. Fluorescence decay parameters for the other nuclease mutants in Table I were also measured. They all have decay parameters that are similar to those for the wild type at 20 °C.

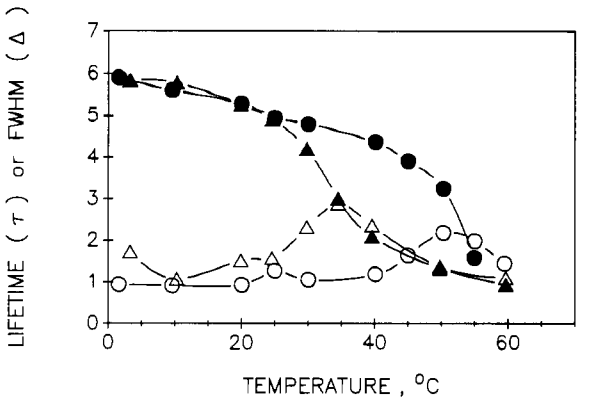

FIGURE 5: Temperature dependence of the mean lifetime, $\bar{\tau}$ (solid symbols), and half-width at half-maximum, Δ (open symbols), for Lorentzian distribution fits to multifrequency phase and modulation data for the nuclease–conA–S28G mutant (▲, △) and wild-type (●, ○) nuclease.

Phase/modulation fluorescence data were obtained for the temperature range 3–60 °C for nuclease–conA–S28G and the wild type. The data display a nonexponential decay in all cases. Fits to a double exponential and to a unimodal Lorentzian distribution of lifetimes [see eqs 1–3 of Eftink et al. (1991)] are shown in Table III. In Figure 5 is plotted the mean lifetime, $\bar{\tau}$, and the half-width at half-maximum, Δ, for a unimodal Lorentzian fit as a function of temperature for the two proteins. Such plots show that the mean lifetime drops in response to the thermal unfolding of the protein. The midpoint of this drop occurs about 20° lower for the mutant than for the wild type. The half-width of the distribution fits also indicates the unfolding transition. The half-width of the forced Lorentzian fits is larger in the temperature range where both folded (long lifetime) and unfolded (short lifetime) components exist. In a future manuscript we will present more extensive lifetime data and analysis.

The midpoint temperatures, of the mean lifetime versus temperature points, are higher than the T_m values from the data in Figure 2. This is due to the fact that the folded state (with its longer lifetime and higher fluorescence intensity) has a disproportionally larger contribution to the average fluorescence lifetime.

Fluorescence lifetime data were also obtained for nuclease–conA–S28G in the presence of 1.5 M urea and at 1330 bar. These conditions are sufficient to induce the respective transitions, as shown in Figures 3 and 4. For both of these perturbations, the mean fluorescence lifetime is reduced to about 1 ns, as is also the case for thermal unfolding. Fits for these fluorescence decays are given in Table III.

Anisotropy Decay Data. Multifrequency differential polarized phase and modulation data were obtained for nuclease–conA–S28G in its native state (20 °C) and for the state that is perturbed by temperature (40 °C), urea (1.5 M), and pressure (1330 bar). Shown in Figure 6 are data for nuclease–conA–S28G at 1 bar and at 1330 bar. Fitting these data [with eq 5 of Eftink et al. (1991)] yields the rotational correlation times in Table IV. More extensive anisotropy decay data will be presented separately, but the present data show that at 20 °C and 1 bar (native state) the anisotropy decay for the mutant is dominated by a rotational correlation time of 11 ns. The temperature, urea, or pressure-induced transitions all result in a large decrease in the rotational correlation time to a value less than 2 ns.

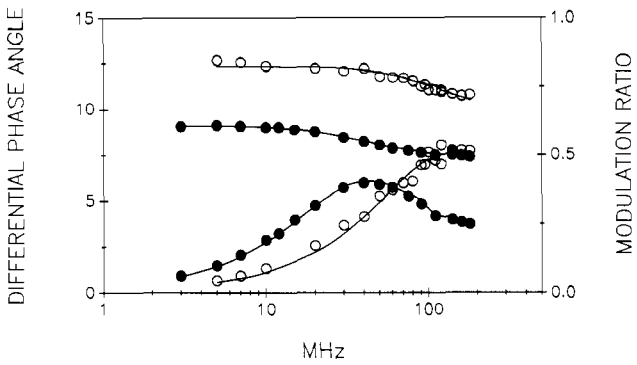

FIGURE 6: Differential polarized phase and modulation data for the anisotropy decay of nuclease–conA–S28G at 1 bar (dark symbols) and at 1330 bar (open symbols). Data collected at 20 °C, pH 7, with excitation at 300 nm. The fits are given in Table IV.

Table IV: Anisotropy Decay Fitting Parameters for Nuclease–conA–S28G[a]

	ϕ_1 (ns)	ϕ_2 (ns)	r_0g_1	r_0g_2	χ^2_R
20 °C	11.3	0.34	0.255	0.02	0.51
1.5 M urea	0.75	*b*	0.194		0.45
1330 bar	1.25	*c*	0.162		4.9
40 °C[d]	1.34	0.08	0.133	0.178	0.8

[a] Data at 20 °C. Excitation at 300 nm. [b] A fixed ϕ_2 of 12 ns was included in the fit to provide for any native protein present. The r_0g_2 recovered for this native component was 0.037, as compared to 0.193 for the 0.75-ns component. This is consistent with there being only a small amount of native nuclease–conA–S28G in the presence of 1.5 M urea. [c] Similarly, a fixed ϕ_2 of 11 ns was included in the fit. The r_0g_2 recovered for this "native" component was 0.012, as compared to 0.162 for the 1.25-ns component. [d] Data taken from work to be published (Eftink et al., 1991).

Discussion

The hybrid mutants, nuclease–conA and nuclease–conA–S28G, have markedly lower thermodynamic stability for their native state, in comparison to wild-type nuclease. The thermal T_m of the hybrid mutants is about 20 °C lower than that for the wild type at pH 7. Whereas the wild type's native state is stabilized (i.e., $\Delta G°_{UN}$) by about 5.8 ± 0.3 kcal/mol at 20 °C, the nuclease–conA and nuclease–conA–S28G mutants are stabilized by only 1.4 ± 0.3 and 1.2 ± 0.2 kcal/mol, respectively, at 20 °C, pH 7. Thus there is a decrease in stability ($\Delta\Delta G°_{UN}$) of about 4.3 and 4.6 kcal/mol respectively for nuclease–conA and S28G, upon substitution of the corresponding hexapeptides into positions 27–31 of nuclease. We have induced the unfolding transition of the hybrid mutants by temperature, pressure, and the denaturants urea and guanidine hydrochloride. Good agreement is found in the $\Delta G°_{UN}$ obtained with each type of perturbation. Each type of transition is well described as a two-state process.

These $\Delta\Delta G°_{UN}$ values are among the largest that have been found for a mutant protein. By comparison, the temperature-sensitive RH96 mutant of T4 lysozyme has a $\Delta\Delta G°_{UN}$ value of 2.83 kcal/mol at pH 6 (a ΔT_m of −7.8 °C) (Becktel & Schellman, 1987).

Since the hybrid mutants of nuclease have such marginal stability, an important question is whether their "native" states are similar to that for the wild type. The crystal structure of nuclease–conA has been determined and comparison to the wild type shows the overall structures to be similar, with only local changes involving positions 27–31 (Hynes et al., 1989). Crystals of nuclease–conA–S28G have also been prepared in the laboratory of R.O.F. and preliminary refinements show this protein to also be similar to the wild type. From these crystallographic studies, a possible explanation for the reduced stability of the hybrids has been suggested to be due to the removal of interactions involving Tyr-27, in the wild type, with Gln-10 (hydrogen bond) and Phe-34 and Phe-76 (hydrophobic interaction) (Hynes et al., 1989).

Our present fluorescence data show the Trp-140 emission spectrum, accessibility to the quencher acrylamide, fluorescence biexponential decay kinetics, and anisotropy decay to be similar for the hybrid mutants and wild-type nuclease A at 20 °C. These results suggest that the native structure of these mutants is like that of the wild type. Also, the hybrid mutants have proton NMR spectra that are similar to that of the wild type and show enzymatic activity, at temperatures below their T_m (Fox et al., results to be published). Therefore, we assume that the "native" state of the hybrid mutants is similar to that of the wild type. The crystal structure of nuclease A shows Trp-140 to be near the end of a long stretch of α-helix. Unfortunately, nearby residues 142–149 are disordered in the crystal, making it difficult to say much about the microenvironment of Trp-140's indole ring in the native state.

Another important question is how to describe the unfolded state of these proteins. It is usually assumed that, under extreme conditions of temperature or denaturant concentration, a protein will unfold to a random coil. With mild denaturing conditions (particularly temperature) it is now thought that unfolded proteins may not be completely in a random coil state but may have some residual structure. Our fluorescence data give information about the environment of Trp-140 in the unfolded state. There is a red shift and large drop in fluorescence intensity and average lifetime of Trp-140 upon unfolding by temperature, solvent denaturants, and pressure (for the hybrid mutants). The red shift indicates an increase in solvent exposure of Trp-140 upon unfolding. The drop in intensity and lifetime is not easily interpreted (although it is certainly advantageous). Presumably, in the unfolded state Trp-140 can experience dynamic quenching by solvent and nearby amino acid residues; such quenching reactions are apparently limited in the folded state, since Trp-140 in nuclease has a relatively long average fluorescence lifetime (and high yield), compared to other Trp residues in proteins (Beechem & Brand, 1985). The rotational correlation time of Trp-140 is found to decrease dramatically as the "unfolding" transition is induced by temperature, solvent denaturant, or pressure. When one extrapolates the thermal transition data back to 20 °C, an apparent rotational correlation time of about 1 ns is found for the unfolded state for each type of transition. Thus, the data indicate that the unfolded state has a solvent-exposed, mobile Trp-140 and that, at least in the segment of the protein containing this residue, the unfolded state behaves as a random coil. Further, each type of unfolding transition appears to produce a similar unfolded state, as sensed by the time-resolved fluorescence of Trp-140.

Registry No. Staphylococcal nuclease, 9013-53-0; urea, 57-13-6; guanidine hydrocloride, 50-01-1.

References

Alexandrescu, A. T., Ulrich, E. L., & Markley, J. L. (1989) *Biochemistry 28*, 204–211.

Antonino, L., Nakano, T., & Fink, A. L. (1989) *J. Cell Biol. 107* (abstract 1136).

Becktel, W. J., & Schellman, J. A. (1987) *Biopolymers 26*, 1859–1877.

Beechem, J. M., & Brand, L. (1985) *Annu. Rev. Biochem. 54*, 43–71.

Borgford, T. J., Gray, T. E., Brand, M. J., & Fehrst, A. R. (1987) *Biochemistry 26*, 7246–7250.

Brochon, J. C., Wahl, P., & Auchet, J. C. (1974) *Eur. J. Biochem. 41*, 577–583.
Cotton, F. A., & Hazen, E. E., Jr. (1971) *Enzymes (3rd Ed.) 4*, 153–175.
Eftink, M. R., & Ghiron, C. A. (1987) *Biophys. J. 52*, 467–473.
Eftink, M. R., Ghiron, C. A., Kautz, R. A., & Fox, R. O. (1989) *Biophys. J. 55*, 575–579.
Eftink, M. R., Ghiron, C. A., Kautz, R. A., & Fox, R. O. (1990) *Proc. SPIE–Int. Soc. Opt. Eng. 1204*, 137–143.
Eftink, M. R., Gryczynski, I., Wiczk, W., Laczko, G., & Lakowicz, J. R. (1991) *Biophys. Chem.* (submitted for publication).
Evans, P. A., Dobson, C. M., Kautz, R. A., Hatfull, G., & Fox, R. O. (1987) *Nature 329*, 266–268.
Fox, R. O., Evans, P. A., & Dobson, C. A. (1986) *Nature 320*, 192–194.
Grinvald, A., & Steinberg, I. Z. (1976) *Biochim. Biophys. Acta 27*, 663–678.
Hansen, D., Altschmied, L., & Hillen, W. (1987) *J. Biol. Chem. 262*, 14030–14035.
Hudson, B., Ruggiero, A., Harris, D., Johnson, T., Dou, X. M., Novet, T., McIntosh, L., Phillips, C., & Nester, T. (1988) *Proc. SPIE-Int. Soc. Opt. Eng. 909*, 113–120.
Hynes, T. R., Kautz, R. A., Goodman, M. A., Gill, J. F., Fox, R. (1989) *Nature 339*, 73–76.
Kautz, R. A., Gill, J. F., & Fox, R. O. (1990) in *Protein and Pharmaceutical Engineering*, pp 1–15, Wiley-Liss, Inc., New York.
Kellis, J. T., Jr., Nyberg, K., Sali, & Fersht, A. R. (1988) *Nature 333*, 784–786.
Kitamura, S., & Sturtevant, J. M. (1989) *Biochemistry 28*, 3788–3792.
Lakowicz, J. R., Laczko, G., Gryczynski, I., & Cherek, H. (1986) *J. Biol. Chem. 261*, 2240–2245.
Matsumura, M., Becktel, W. J., & Matthews, B. W. (1988) *Nature 334*, 406–410.
Matthews, B. (1987) *Biochemistry 26*, 6885–6888.
Matthews, B. W., Nicholson, H., & Becktel, W. J. (1987) *Proc. Natl. Acad. Sci. U.S.A.*
Oxender, D. L., & Fox, C. F. (1987) *Protein Engineering*, Alan R. Liss, Inc., New York.
Pace, C. N., Shirley, B. A., & Thomson, J. A. (1989) in *Protein Structure and Function: A Practical Approach* (Creighton, T. E., Ed.) pp 311–330, IRL Press, Oxford, England.
Schellman, J. A. (1978) *Biopolymers 17*, 1305.
Serpersu, E. H., McCracken, J., Peisach, J., & Mildvan, A. S. (1988) *Biochemistry 27*, 8034–8044.
Shortle, D., & Meeker, A. K. (1986) *Proteins: Struct., Funct., Genet. 1*, 81–89.
Shortle, D., Meeker, A. K., & Freire, E. (1988) *Biochemistry 27*, 4761–4768.
Waldman, A. D. B., Clarke, A. R., Wigley, D. G., Hart, K. W., Chia, W. N., Barstow, D., Atkinson, T., Munro, I., & Holbrook, J. J. (1987) *Biochim. Biophys. Acta 913*, 66–71.
Weaver, L. A., Gray, T. M., Grutter, M. G., Anderson, D. E., Wozniak, J. A., Dahlquist, F. W., & Matthews, B. W. (1989) *Biochemistry 28*, 3793–3797.
Zipp, A., & Kauzmann, W. (1973) *Biochemistry 12*, 4217–4228.

Internal Intensity Standards for Heme Protein UV Resonance Raman Studies: Excitation Profiles of Cacodylic Acid and Sodium Selenate†

Sunho Song and Sanford A. Asher*
Department of Chemistry, University of Pittsburgh, Pittsburgh, Pennsylvania 15260
Received July 18, 1990; Revised Manuscript Received October 9, 1990

ABSTRACT: We examine the utility of SO_4^{2-}, ClO_4^-, cacodylic acid, and SeO_4^{2-} as internal intensity standards for Raman spectral measurements of protein structure. We find that 0.1 M SO_4^{2-} and ClO_4^- perturb the protein tertiary structure of aquomethemoglobin (met-Hb) and its fluoride (met-HbF) and azide (met-HbN_3) complexes. Changes occur for the tryptophan near-UV absorption bands, the iron spin state is altered, and the fluoride ligand affinity decreases. Concentrations of ClO_4^- and SO_4^{2-} as low as 0.1 M suppress the met-HbF quaternary R → T transition induced by the allosteric effector inositol hexaphosphate (IHP). In contrast, similar concentrations of cacodylic acid and SeO_4^{2-} show little effect on the hemoglobin tertiary or quaternary protein structures or upon the R → T transition induced by IHP. We measure the Raman cross sections of cacodylic acid and SeO_4^{2-} between 218 and 514.5 nm and find that for UV excitation they are ca. 5-fold larger than ClO_4^- or SO_4^{2-}. Thus, cacodylic acid and selenate can be used at lower concentrations. Cacodylic acid and SeO_4^{2-} are superior Raman internal intensity standards for protein structural studies.

The use of resonance Raman spectroscopy for biomolecular studies has recently been extended into the UV region in order to probe aromatic chromphores such as aromatic amino acids in proteins and nucleic acid bases (Asher, 1988). For example, recent applications have included studies of tyrosine and tryptophan in hemoglobin (Song & Asher, 1990; Asher, 1988; Kaminaka et al., 1990; Su et al., 1989), in myoglobin (Harmon et al., 1990; Larkin et al., 1990a), and in bacteriorhodopsin (Harada et al., 1990) as well as other proteins [see Sweeney et al. (1990), Asher (1988), and Harada and Takeuchi (1986) and references cited therein]. In these studies, significant environmental information derives from the Raman intensities. The intensity information is generally obtained from Raman

† This work was supported by NIH Grant IR01GM30741-09.
* Author to whom correspondence should be addressed.

0006-2960/91/0430-1199$02.50/0